19th Symposium IMEKO TC 4 Symposium and 17th IWADC Workshop
Advances in Instrumentation and Sensors Interoperability
July 18-19, 2013, Barcelona, Spain

Defining frequency domain performance of Analog-to-Information converters

Doris Bao, Pasquale Daponte, Luca De Vito, Sergio Rapuano

Department of Engineering, University of Sannio, Piazza Roma, 21, 82100, Benevento, Italy,
ph: +39 0824 305600, fax: +39 0824 305840,
{doris.bao, daponte, devito, rapuano}@unisannio.it

Abstract **-** The paper deals with the definition of dynamic performance of Analog-to-Information Converters (AICs). These components allow of overcoming the sampling frequency limits of the Shannon's theorem, by assuming that the observed signal has a sparse representation in a given domain. The paper aims to verify the behavior of standard parameters currently defined for Analog-to-Digital Converters when applied to the AICs. To this aim, several simulations and experimental tests have been carried out to study the influence, in the frequency domain, of quantization noise and nonlinearity on the AIC dynamic parameters.

I. Introduction

Recent studies about Compressed Sensing (CS) theory demonstrate that it is possible to recover a signal from fewer samples than those required in Shannon's theorem, when the signal is sparse or compressible in some transform domain [1], [2]. Based on these emerging CS techniques, some architectures of Analog-to-Information Converters (AICs) have been proposed. They could become an alternative to conventional Analog-to-Digital Converters (ADCs) in applications where the signal information is concentrated in a limited number of high frequencies [3]. For example, some important radar and communication applications require high sampling rates, but, since even high resolutions are needed, their requirements cannot be achieved by current ADCs [4].
The idea, underlying the AIC is to spread the frequency content of the input signal such that the high frequency components are folded back to low frequencies, in order to pass the anti-aliasing filter of the subsequent ADC, having a lower sampling frequency than that required by the Shannon's theorem for the original signal. The architectures proposed to realize the AIC concept are basically three, each implementing the frequency spreading by exploiting: (i) non-uniform [5] or random sampling [6], (ii) random filters [7], and (iii) random demodulation [4].
The aim of the research is to define performance parameters and test methods for AICs, starting from the state of art of research and the scientific knowledge about ADC testing. To this aim, the first step is the application to AICs of standard parameters and test methods, actually defined for ADCs in order to study how they are influenced by (i) the AIC architecture type, (ii) the AIC design parameters, and (iii) the circuit non-idealities.
In the scientific literature few papers can be found, facing the AIC testing and most of them take into account only a reduced set of figures of merits and influencing parameters [8].
This paper has the aim of defining the performance of an AIC to reconstruct an input signal that is sparse in the frequency domain. Therefore, the behavior of the dynamic parameters in the frequency domain, such as Signal to Noise Ratio (SNR), Signal to Noise and Distortion Ration (SINAD), Total Harmonic Distortion (THD) and Spurious Free Dynamic Range (SFDR) has been observed, when some of the influencing parameters are varied, such as the ADC resolution and nonlinearity, and the test signal frequency.
To this aim, first, simulation tests have been carried out, by modeling nonlinearity and quantization of the ADC included in the AIC. Then, experimental tests have been carried out on an AIC prototype.
The AIC architecture considered in this paper is based on the random demodulation, as it does not require a high sampling frequency ADC. However, test methods and considerations can be easily extended to the other types of AIC architectures.
The paper is organized as it follows: In Section II, an introduction of the random demodulation AIC architecture is given. Then, in Section III and Section IV, the results of the simulation and experimental evaluation phases are reported and discussed, respectively.

II. The random demodulation AIC architecture

A block scheme of the random demodulation AIC architecture is shown in Fig.1. Considering an observation window with a duration Δt, the analog signal to be acquired $x(t)$, defined in the time window, having a Nyquist

ISBN-10: 84-616-5438-2 | ISBN-13: 978-84-616-5438-3

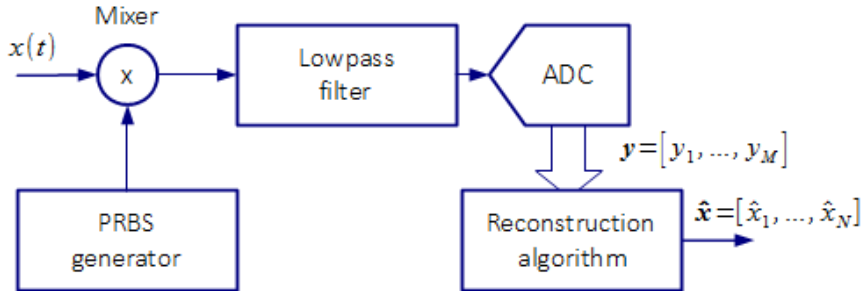

Fig. 1. Block diagram of the random demodulation AIC architecture.

frequency equal to f_p, would need a sampling frequency at least of $F_s=2f_p$, if acquired according with the Shannon's theorem, and would give in this case a vector of $N= \Delta t\, F_s$ samples $\mathbf{x} = [x_1, \ldots, x_N]$.
Instead of directly sampling it, $x(t)$ is mixed with a Pseudo-Random Binary Sequence (PRBS), having a bit rate equal to or greater than f_p. This mixing process allows of spreading the harmonic content of the signal, so that at least a spectral replica falls within the Nyquist band ($[0, f_s/2]$ Hz) of the following ADC. Then, the mixed signal is low-pass filtered and digitized using a sampling frequency f_s lower than F_s, giving as output a vector of $M= \Delta t\, f_s$ samples $\mathbf{y} = [y_1, \ldots, y_M]$, where $M < N$.
The low-pass filter is in charge of avoiding aliases [10]. Finally, a reconstruction algorithm allows of obtaining an estimate $\hat{\boldsymbol{x}}$, from the elements of the vector $\mathbf{y}$, which represents an undersampled version of $\mathbf{x}$.
The reconstruction algorithm should solve one of the following optimization problems:

$$\hat{\mathbf{x}} = argmin \|\mathbf{x}\|_1 \quad \text{s. t.} \quad \mathbf{y} = \boldsymbol{\Phi}\boldsymbol{\Psi}\boldsymbol{x}\,, \tag{1}$$

or

$$\hat{\mathbf{x}} = argmin \|\mathbf{x}\|_1 \quad \text{s. t.} \quad \|\mathbf{y} - \boldsymbol{\Phi}\boldsymbol{\Psi}\boldsymbol{x}\|_\infty < \varepsilon\,, \tag{2}$$

where, $\boldsymbol{\Phi}$ is the matrix modeling the mixing and filtering blocks, $\boldsymbol{\Psi}$ is the matrix modeling the Fourier Transform, $\|.\|_1$ and $\|.\|_\infty$ are the l_1 and l_∞ norms.
The former problem contains an equality constraint while the latter problem relaxes the constraint to an inequality that allows of considering noise and nonlinearity. In this case, ε determines the number of frequency components to be detected in the input signal. In order to reconstruct a sparse signal in the frequency domain, the AIC should identify only the components of the input signal, and discard those corresponding to noise and nonlinearity. In this case, ε should be chosen greater than the squared root of the sum of the powers of noise and nonlinearity [8].

III. Simulation tests

During simulation phase, the mixing and filtering blocks of the AIC have been modeled as a matrix multiplication, as shown in [10]. Therefore, as suggested in [10], a diagonal matrix **D**, having as elements the values of the PRBS, and a matrix **H** from the impulse response of the filter, have been computed. Matrix $\boldsymbol{\Phi}$ has been then obtained as:

$$\boldsymbol{\Phi} = \boldsymbol{M}\,\boldsymbol{D} \tag{3}$$

Instead, the ADC has been modeled as a sequence of nonlinearity and quantization, where the nonlinearity has been obtained, as in [8], using the following third order polynomial function:

$$f(a) = \frac{a + c_3 a^3}{1 + c_3} \tag{4}$$

The Dantzig selector [11] has been used as reconstruction algorithm, solving the optimization problem in (2), as it is implemented in the l1-magic Matlab toolbox [12], for both the simulation and the following experimental phase.
In order to verify the behavior of the standard parameters in the frequency domain, simulation tests have been performed on a sine wave acquired using 100 blocks, each with N=256 samples, by using a bit rate of the PRBS equal to 200Mbit/s and the ADC sampling frequency equal to f_s=50 MSa/s. According to the assumptions made

ISBN-10: 84-616-5438-2 | ISBN-13: 978-84-616-5438-3

above this choice allows a Nyquist frequency of the equivalent ADC f_p = 200 MSa/s
An estimate of the output signal Power Spectral Density (PSD), obtained by averaging the Fast Fourier Transforms (FFTs) of the 200 acquired blocks has been used to estimate the frequency domain parameters.
Several tests have been performed for different values of: (i) the test signal frequency, (ii) the nonlinearity parameter c3, (iii) the ADC resolution, (iv) the undersampling ratio $f_s/2f_p$, and (v) the parameter ε. Some of the obtained results are presented in the following Sub-Sections.

A. Dynamic figures of merit vs. test signal frequency
These tests have been carried out with undersampling ratio to 1/4, resolution to 10 bits, modeled using an ideal quantizer, followed by the nonlinearity in (4), with c_3 = 0.2, ε = 0.01, and the test signal frequency ranging in the range from 10 MHz to 90 MHz, with a step of 10 MHz.
The results, reported in Fig. 2, show a decrease of the performance around 50 MHz, due to an exact overlapping of some signal higher order harmonics.

B. Dynamic figures of merit vs. nonlinearity
In this case, test signal frequency has been fixed to 10.16 MHz, and ε equal to 0.1, while the nonlinearity parameter c_3 has been varied in the set {0.05, 0.1, 0.2, 0.5, 1, 2, 5, 10}. Results are shown in Fig.3, for two cases, when no quantization has been introduced (square markers) and when a 10 bit resolution is used (diamond markers). A relevant aspect is that a nonlinearity increase affects not only the frequency bins where the signal harmonics are located, but an increase of the noise floor has been observed, too, even if the quantization noise remains unchanged. This behavior can be easily observed in Fig.3d, where the SNR is reported, which shows a trend very similar to the SINAD reported in Fig.3b. This is probably due to the spreading of the harmonic content introduced by the mixing with the PRBS sequence. By taking into account this aspect, a redefinition of the THD or different interpretation of its value is needed for AICs.

C. Dynamic figures of merit vs. parameter ε
These tests have been carried out using a test signal frequency fixed to 21.06 MHz, nonlinearity parameter c_3 equal to 0.2 and ADC resolution set to 10 bits. The results, reported in Fig. 4, show an increase of the performance with ε, since a higher value of ε allows discarding a greater number of components from the reconstructed signal. Since, in this case, a single sinewave signal is used, the discarded components always belong to noise and distortion.
Although in the practical case, ε should be chosen greater than the squared root of the sum of the powers of noise and ADC nonlinearity, it is important for the AIC testing purpose to know how the dynamic figures of merit behaves at lower values of ε, in order to observe how nonlinearity and noise component will affect the component.

IV. Preliminary experimental evaluation

A preliminary experimental phase has been carried out, by setting up an AIC prototype. It is composed by: (i) an AD8342-EVALZ mixer evaluation board from Analog Devices, (ii) a Tektronix TDS5104B oscilloscope which realizes the filter and the Analog to Digital conversion, and (iii) a laptop computer that executes the reconstruction algorithm. The computer controls a Tektronix AWG420 Arbitrary Waveform Generator, which generates the PRBS, and an Agilent E4438C signal generator, which generates the test signal.
A 10 MHz reference signal has been used to synchronize the Agilent E4438C, the Tektronix AWG420 signal generators and the Tektronix TDS5104B oscilloscope, in order to guarantee the coherent sampling condition,

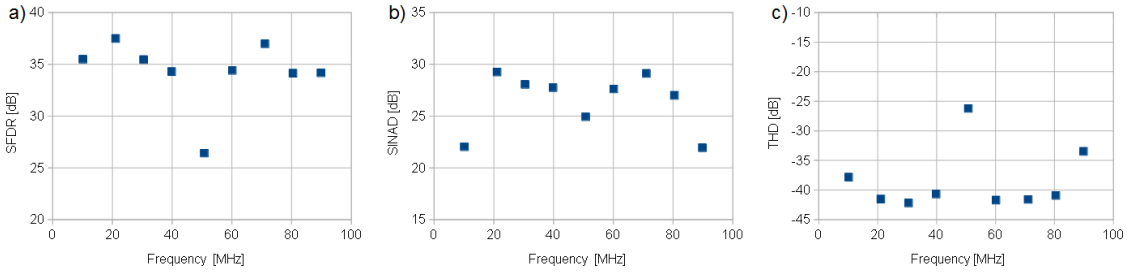

Fig. 2. Simulation results of SFDR (a), SINAD (b) and THD (c) obtained for values of the input test frequency ranging from 10 to 90 MHz.

ISBN-10: 84-616-5438-2 | ISBN-13: 978-84-616-5438-3

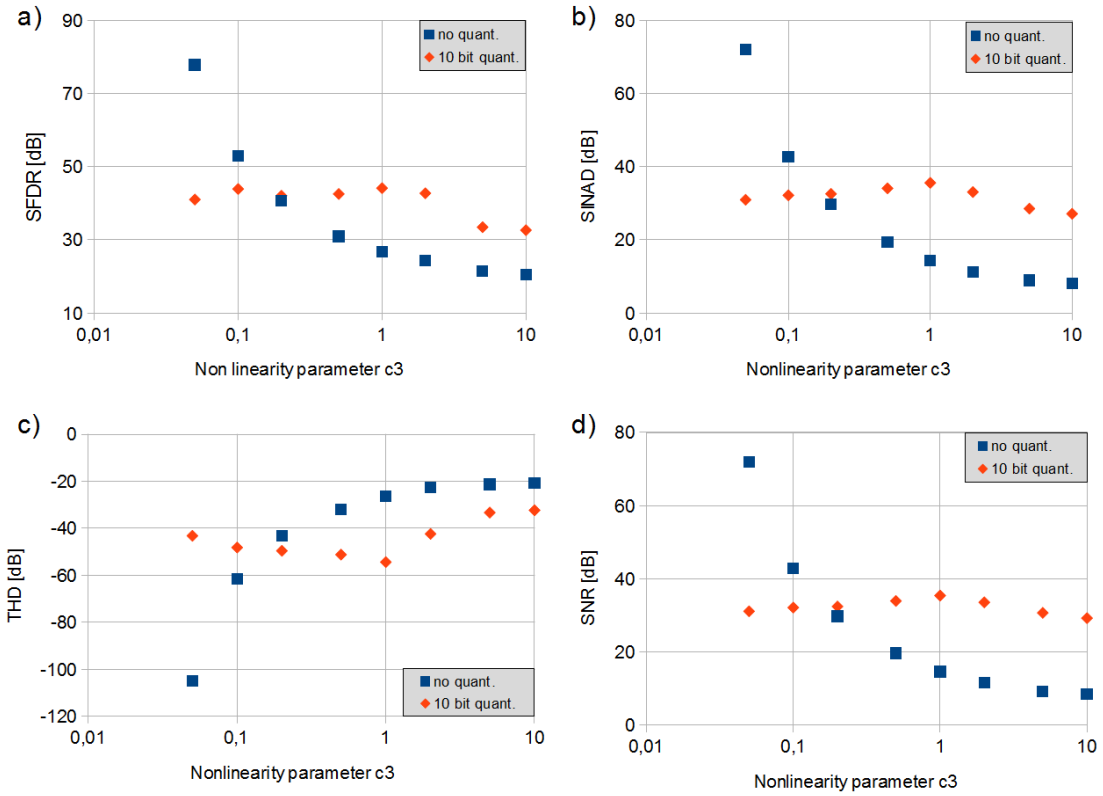

Fig. 3. Simulation results of SFDR (a), SINAD (b), THD (c) and SNR (d), obtained by varying the nonlinearity parameter c_3, without quantization (square markers) and when a 10 bit resolution quantization is applied (diamond markers).

while the CH1 MARKER OUT line of the Tektronix AWG420 is used to trigger the oscilloscope to the beginning of the PRBS.
The whole laboratory setup is shown in Fig. 5. Since a minimal resolution is needed for the signal reconstruction, the oscilloscope resolution has been increased by oversampling and averaging the samples by a factor of 25, thus bringing the resolution to about 10.3 bits. Therefore, the sampling frequency of the oscilloscope has been set to 1.25 GSa/s, giving an equivalent sampling frequency of 50 MSa/s. The bit-rate of the PRBS has been set to 200 Mbit/s. For the test purposes, sinewave test signals have been generated with frequency ranging from 5 MHz to 95 MHz, and the figures of merit have been evaluated on spectra obtained averaging the FFTs obtained from 200 records, each 512 samples long.

A. Dynamic figures of merit vs. epsilon
In Fig. 6 the results of the figures of merit vs. the reconstruction parameter ε are shown. As it can be seen, the

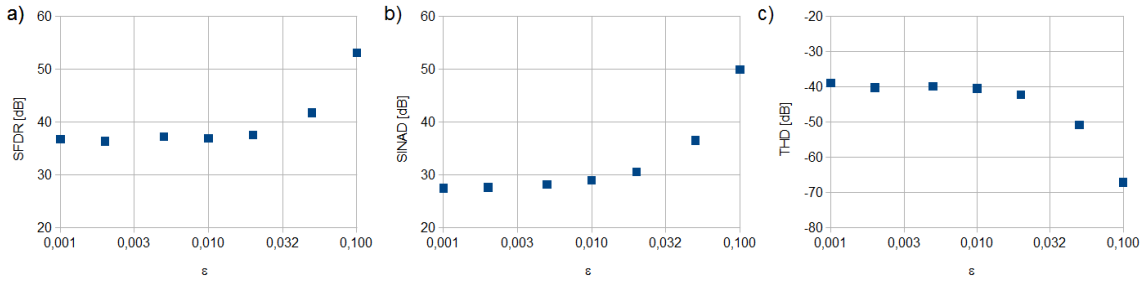

Fig. 4. Simulation results of SFDR (a), SINAD (b) and THD (c) obtained by varying the reconstruction parameter ε in the set {0.001, 0.002, 0.005, 0.01, 0.02, 0.05, 0.1}.

ISBN-10: 84-616-5438-2 | ISBN-13: 978-84-616-5438-3

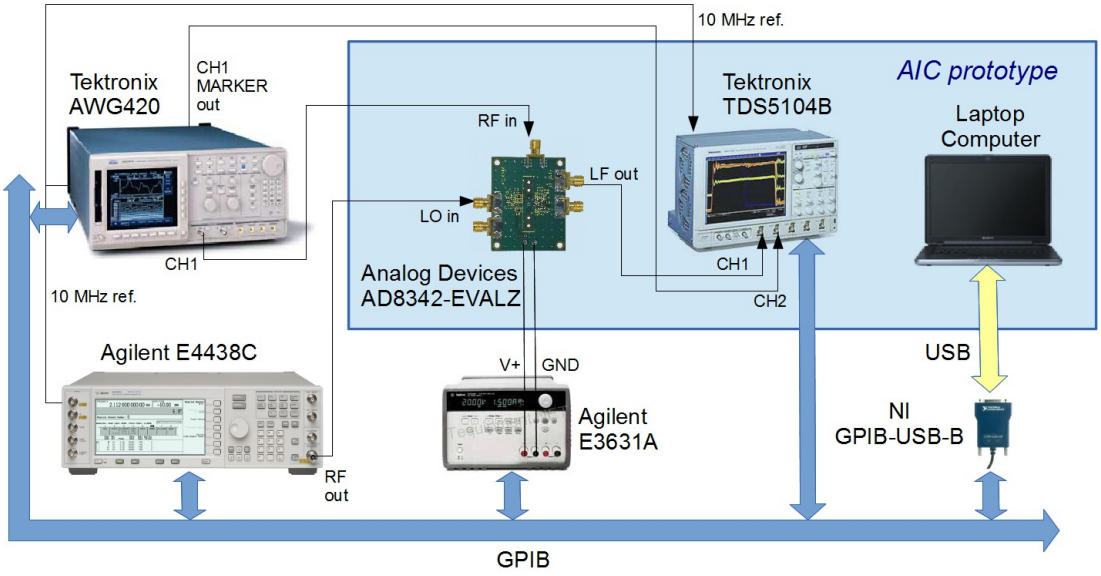

Fig. 5. Laboratory setup for the experimental tests.

AIC performance increases with ε, since a higher value of ε allows excluding a higher number of noise and distortion components.

B. Dynamic figures of merit vs. test signal frequency

In Fig. 7, some results, showing the trend of the AIC figures of merit versus the input signal frequency are given. In this case, it can be noted a performance improvement with the frequency, mainly reported by the SINAD and the THD, due to a lowpass behavior of the system, that filters out some higher order harmonics.

It can be noted that the reduction of performance around 50 MHz, observed in simulation, is not more observable in experimental results, probably due to the noise that avoids the exact overlapping of some unwanted components.

V. Conclusions and further work

In this paper, the definition of parameters and test methods for AICs has been faced, by evaluating the behavior of standard figures of merit when some of the AIC influencing parameters have been taken into account. The analysis has been conducted on the random demodulation architecture, first in simulation, where it was possible to change even the resolution and the nonlinearity of the internal ADC, and then in an experimental phase, on a AIC prototype. The results showed that figures of merit evaluated in the frequency domain, actually defined for ADCs, could generally be used to metrologically characterize random demodulation AICs. However, attention should be paid to the use of the THD, since the energy of signal harmonics is not more concentrated to few spectral lines, but is spread all over the observed band. In addition, the figures of merit should be evaluated for several values of the reconstruction parameter ε, since high values of ε can hide the effects of noise and distortion.

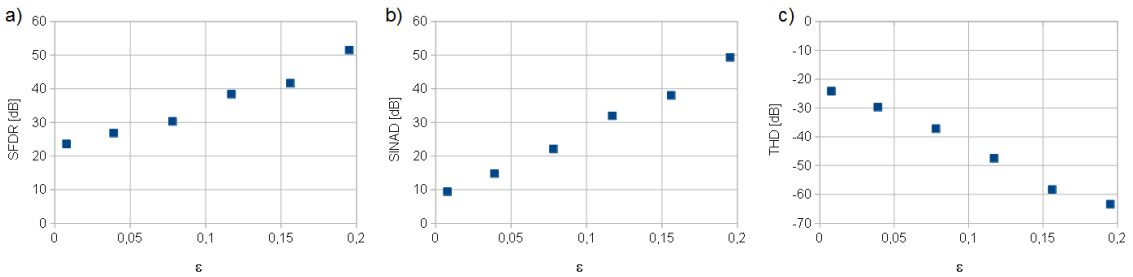

Fig. 6. Trend of SFDR (a), SINAD (b), and THD (c), versus the parameter ε in the set {0.01, 0.04, 0.08, 0.12, 0.16. 0.20}.

ISBN-10: 84-616-5438-2 | ISBN-13: 978-84-616-5438-3

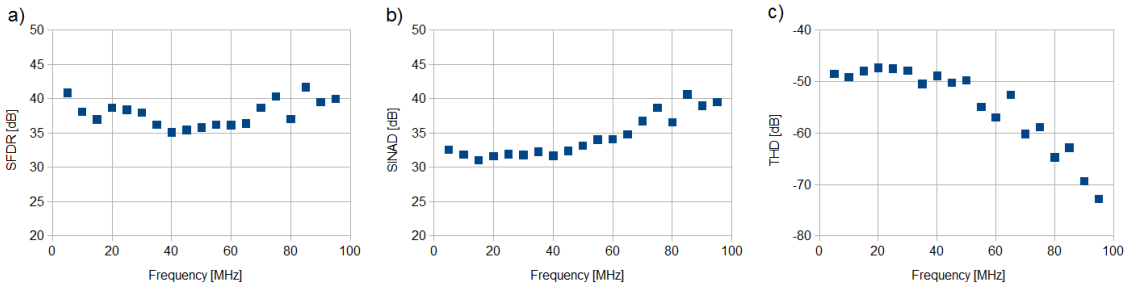

Fig. 7. Trend of SFDR (a), SINAD (b), and THD (c), versus the input signal frequency, ranging from 5 to 95 MHz.

Further work is directed to a deeper experimental investigation, by using an ADC circuit instead of the oscilloscope, thus removing the need of oversampling and averaging. Moreover, the analysis should be extended to other AIC architectures, such that based on random sampling, and to the figures of merit evaluated in the time domain.

References

[1] D.L.Donoho, "Compressed sensing", IEEE Trans. on Information Theory, vol.52, No.4, April 2006, pp.1289–1306.

[2] E.J.Candes, M.B.Wakin, "An introduction to compressive sampling", IEEE Signal Processing Magazine, vol.25, March 2008, pp.21–30.

[3] O.Abari, F.Chen, F.Lim, V.Stojanovic, "Performance trade-offs and design limitations of analog-to information converter front-ends", IEEE Int. Conf. on Acoustics, Speech and Signal Processing, March 2012, pp.5309-5312.

[4] S.Kirolos, J.Laska, M.Wakin, M.Duarte, D.Baron, T.Ragheb, Y.Massoud, R.Baraniuk, "Analog-to-information conversion via random demodulation", Proc. of 2006 IEEE Dallas/CAS Workshop on Design, Applications, Integration and Software, Oct. 2006, pp.71–74.

[5] M.Wakin, S.Becker, E.Nakamura, M.Grant, E.Sovero, D.Ching, J.Yoo, J.Romberg, A.Emami-Neyestanak, E.Candes, "A nonuniform sampler for wideband spectrally-sparse environments", IEEE Journal on Emerging and Selected Topics in Circuits and Systems, vol.2, No.3, Sept. 2012, pp. 516–529.

[6] J.Laska, S.Kirolos, "Random sampling for analog-to-information conversion of wideband signals", Proc. of IEEE Dallas/CAS Workshop on Design, Applications, Integration and Software, Oct. 2006, pp.119–122.

[7] J.A.Tropp, M.B.Wakin, M.F.Duarte, D.Baron, R.G.Baraniuk, "Random filters for compressive sampling and reconstruction", Proc. of 2006 IEEE Int. Conf. on Acoustics Speed and Signal Processing, vol.3, pp.III–872–III–875.

[8] Z.Yu, J.Zhou, M.Ramirez, S.Hoyos, B.M.Sadler, "The impact of ADC nonlinearity in a mixed-signal compressive sensing system for frequency-domain sparse signals", Physical Communication, vol.5, No.2, June 2012, pp.196–207.

[9] "IEEE Standard for Terminology and Test Methods for Analog-to-Digital Converters", IEEE Std.1241-2010 (Revision of IEEE Std.1241-2000).

[10] J.Tropp, J.Laska, "Beyond Nyquist: Efficient sampling of sparse bandlimited signals", IEEE Trans. on Information Theory, vol.56, No.1, 2010, pp.520–544.

[11] E.Candes, T.Tao, "The Dantzig selector: Statistical estimation when p is much larger than n", The Annals of Statistics, vol.35, No.6, Dec. 2007, pp.2313–2351.

[12] l1-magic toolbox, http://users.ece.gatech.edu/~justin/l1magic/.

ISBN-10: 84-616-5438-2 | ISBN-13: 978-84-616-5438-3